

Summary. The Common-Reflection-Surface (CRS) stack as an alternative to conventional stacking methods has so far mainly been applied to single-component data. We introduce an approach that allows to generate separate stacks of compressional and transversal waves from multi-component seismic reflection data. Based on the traveltimes approximation for finite offset, the polarization is analyzed during the search for the optimum orientation and curvature of the CRS stacking operator. We apply this approach to a simple synthetic data set and obtain stacked sections and kinematic wavefield attribute sections separately for PP and PS reflection events.

Introduction. The CRS stack was originally developed to stack single-component prestack data acquired along one straight line into a 2D zero-offset (ZO) section. This technique is referred to as 2D ZO CRS stack, see for instance Mann et al. (1999) and Müller (1999). Zhang et al. (2001) extended the CRS stack in order to stack 2D prestack data into a selected finite-offset (FO) gather rather than into a ZO section. If this FO gather is a common-offset (CO) gather this method is referred to as 2D CO CRS stack (Bergler, 2001). In this case the moveout surfaces are described by five kinematic wavefield attributes rather than by three in the ZO case. The search for the wavefield attributes is performed by means of coherence analyses in the prestack data volume. Thus, a velocity model of the subsurface is not required to perform the stack except from the near-surface velocities at the sources and receivers in order to calculate wavefield attributes with a geometrical meaning and to compute the search ranges for the attributes.

Bergler (2001) showed that the 2D CO CRS stacking operator can be used to describe traveltimes of PS converted waves by choosing a P-wave velocity at the sources and a S-wave velocity at the receivers. Moreover, Bergler et al. (2002) discussed the application of the 2D CO CRS stack to data that were acquired with two components (vertical and horizontal). However, in this approach the CRS stack was performed with both components separately and the distinction between PP and PS reflection events was achieved after the CRS stack.

The objective of this paper is to show that the 2D CO CRS stack is able to distinguish between both wave types during the CRS stack to obtain a PP and a PS CO CRS stacked section and five kinematic wavefield attribute sections for each of the both wave types. This is demonstrated with a simple synthetic 2D land data set where vertical and horizontal components have been simulated.

CO CRS stacking operator. This operator approximates the traveltimes of a reflection event in the vicinity of an arbitrarily selected point (t_0, x_0, h_0) on the reflection event. t_0 denotes the traveltimes at the selected point, x_0 the midpoint between source and receiver associated with this point, h_0 is their half-offset. For any other trace located at (x, h) in the vicinity of (x_0, h_0) , the hyperbolic traveltimes approximation (Bergler, 2001; Zhang et al., 2001) reads

$$t^2(\Delta x, \Delta h) = \left[t_0 + \left(\frac{\sin \beta_G}{v_G} - \frac{\sin \beta_S}{v_S} \right) \Delta x + \left(\frac{\sin \beta_G}{v_G} + \frac{\sin \beta_S}{v_S} \right) \Delta h \right]^2 + t_0 \left[2\Delta h \Delta x \left(K_3 \frac{\cos^2 \beta_G}{v_G} + K_2 \frac{\cos^2 \beta_S}{v_S} \right) + \Delta x^2 \left((4K_1 - 3K_3) \frac{\cos^2 \beta_G}{v_G} - K_2 \frac{\cos^2 \beta_S}{v_S} \right) + \Delta h^2 \left(K_3 \frac{\cos^2 \beta_G}{v_G} - K_2 \frac{\cos^2 \beta_S}{v_S} \right) \right], \quad (1)$$

where the midpoint and offset displacements are defined as $\Delta h = h - h_0$ and $\Delta x = x - x_0$, respectively. The near-surface velocities of the considered wave type are denoted by v_S and v_G at source and receiver, respectively. The remaining five parameters are the so-called kinematic wavefield attributes. They are related to propagation directions and curvatures of wavefronts: β_S and β_G are the incidence/emergence angles of the central ray at source and receiver, respectively. The wavefront curvature K_1 observed at the receiver is due to an (actual) common-shot (CS) experiment, whereas K_2 and K_3 are curvatures of wavefronts related to a hypothetical common-midpoint (CMP) experiment, again measured at source and receiver, respectively. A detailed discussion of these wavefront properties can be found in Bergler (2001).

In the CRS stack for single-component data, the optimum set of wavefield attributes is determined by means of coherence analyses along the stacking operator (1) similar to a conventional stacking velocity analysis. Although originally derived for surface seismic geometries, this traveltime approximation also holds for OBS geometries with virtually horizontal sea floor (see separate contribution).

Including polarization information. Assuming an isotropic layer below the receiver line, the polarization directions of P and S waves emerging at the receivers are directly related to the propagation direction of the emerging wavefront (which might be hypothetical). For the receiver associated with the central ray, this direction is given by the wavefield attribute β_G . However, for any other trace within the stacking aperture, this direction will, in general, be different. Thus, it has to be extrapolated from the (known) attributes associated with the central ray. In the second-order approximation inherent to the CRS stack approach, we can assume the radius of curvature $R_G = 1/K_G$ of the emerging wavefront at the receiver to be constant within the stacking aperture. Thus, the emergence angle γ of a paraxial ray can be extrapolated by (modified after Höcht et al., 1999)

$$\sin \gamma = \text{sgn}(R_G) \frac{R_G \sin \beta_G + \Delta x_G}{\sqrt{R_G^2 + 2R_G \Delta x_G \sin \beta_G + \Delta x_G^2}}, \quad (2)$$

where Δx_G is the horizontal displacement between the receiver of the central ray and the receiver of the considered paraxial ray (see Figure 1). Note that K_G depends on the considered source/receiver configuration. It is given by a linear combination of the two curvatures K_1 and K_3 (not shown) defined at the receiver. Equation (2) does not consider the free surface or the effect of the seafloor in OBS data. Appropriate corrections are required in such situations.

Implementation strategy. For a given set of the five wavefield attributes, R_G and γ can always be calculated (the singularity of Equation (2) for the common-receiver gather, $R_G = \Delta x_G = 0$, is removable). The angle γ allows to extract the longitudinal and transversal components from the multi-component data for the coherence analysis as well as the stack. A simultaneous search for all five parameters is quite time consuming. Therefore, the global optimization problem is often decomposed into several (global) optimization steps performed with subsets of the entire prestack data, optionally followed by a local optimization with the full, spatial operator. For the CO CRS stack, Bergler (2001) implemented such a search strategy which starts with a two-parameter search in the CMP gather. However, the need to determine R_G and γ during the stack requires a different search strategy:

- Search for β_G and K_1 in the CS gather. In this case $K_G = K_1$ such that γ is always well defined. This yields separate CS-stacked CO sections for PP and PS waves.

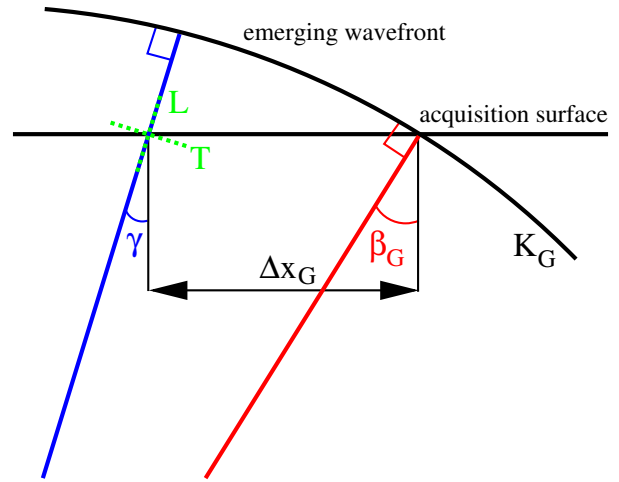


Figure 1: Definition of emergence angles for central (red) and paraxial (blue) ray. The expected transversal (T) and longitudinal (L) polarization directions are indicated in green.

- Two successive one-parameter searches (or alternatively one two-parameter search) in the simulated CO sections. This yields the second angle β_S and a combination of K_1 , K_2 , and K_3 . Polarization does not have to be considered, as the PP and PS events are already separated in the simulated CO sections.
- A final one-parameter search in the CMP gather for a combination of K_2 and K_3 . This search is performed in the multi-component data. Thus, polarization has to be considered with $K_G = K_3$.
- Stack along the full spatial operator in the full prestack data set. For each contributing trace, K_G is given by a linear combination of K_1 and K_3 . This yields the final CRS-stacked CO sections for PP and PS reflections.

A first data example. To evaluate our approach, the proposed strategy was applied to a very simple synthetic 2D land data set. The model (not shown) consists of a single horizontal reflector at a depth of 2 km. P-wave velocity v_P is 2 km/s, S-wave velocity v_S is $v_P/\sqrt{3}$. Shot spacing is 25 m, receiver spacing 50 m. The modeled multi-component prestack data contains the primary PP and PS reflections with a zero-phase Ricker wavelet, peak frequency 30 Hz, and a sampling interval of 4 ms. Free-surface effects have not been modeled. Figure 2 shows the horizontal and vertical components for half-offset $h = 500$ m. Both events are present on both components. Figure 3 shows a subset of the CO sections obtained after search and stack in the CS section together with the associated coherence sections for PP and PS events. This first step is already sufficient to completely separate the PP and PS events, the successive processing steps further increase the signal to noise ratio due to the spatial stacking operator. Note that the resulting CO sections represent the longitudinal or transversal component of the data with respect to the determined stacking operator, i. e., the direction of particle displacement will, in general, vary from event to event as well as along events.

Conclusions & outlook. We have presented a new approach to handle multi-component data by means of the 2D CO CRS stack. This approach is able to distinguish between PP and PS reflections by combining operator shape and orientation with polarization information. It provides stacked sections and kinematic wavefield attribute sections separately for both wave types. An application to a simple synthetic land data set demonstrated that the approach is able to detect, clearly separate, and locally parameterize PP and PS events during the stack. Note that OBS data can be readily processed with the same strategy in case of a virtually horizontal seafloor.

The proposed approach can also be applied to other multi-component acquisition schemes like land seismic data or OBS data with varying surface/seafloor elevation or VSP data. In these cases, different CRS stacking operators are required to approximate the reflection traveltimes, but the handling of polarization information remains the same. Tests with more realistic models for land and OBS geometries are currently in progress.

Acknowledgments

We would like to thank the sponsors of the *Wave Inversion Technology Consortium* for their support.

References

- Bergler, S. (2001). The Common-Reflection-Surface Stack for Common Offset - Theory and Application. Master's thesis, University of Karlsruhe.
- Bergler, S., Duveneck, E., Höcht, G., Zhang, Y., and Hubral, P. (2002). Common-Reflection-Surface stack for converted waves. *Stud. geophys. geod.*, 46:165–175.
- Höcht, G., de Bazelaire, E., Majer, P., and Hubral, P. (1999). Seismics and optics: hyperbolae and curvatures. *J. Appl. Geoph.*, 42(3,4):261–281.
- Mann, J., Jäger, R., Müller, T., Höcht, G., and Hubral, P. (1999). Common-Reflection-Surface stack – a real data example. *J. Appl. Geoph.*, 42(3,4):301–318.
- Müller, T. (1999). *The Common Reflection Surface stack method – seismic imaging without explicit knowledge of the velocity model*. Der Andere Verlag, Bad Iburg.
- Zhang, Y., Bergler, S., and Hubral, P. (2001). Common-Reflection-Surface (CRS) stack for common-offset. *Geophys. Prosp.*, 49(6):709–718.

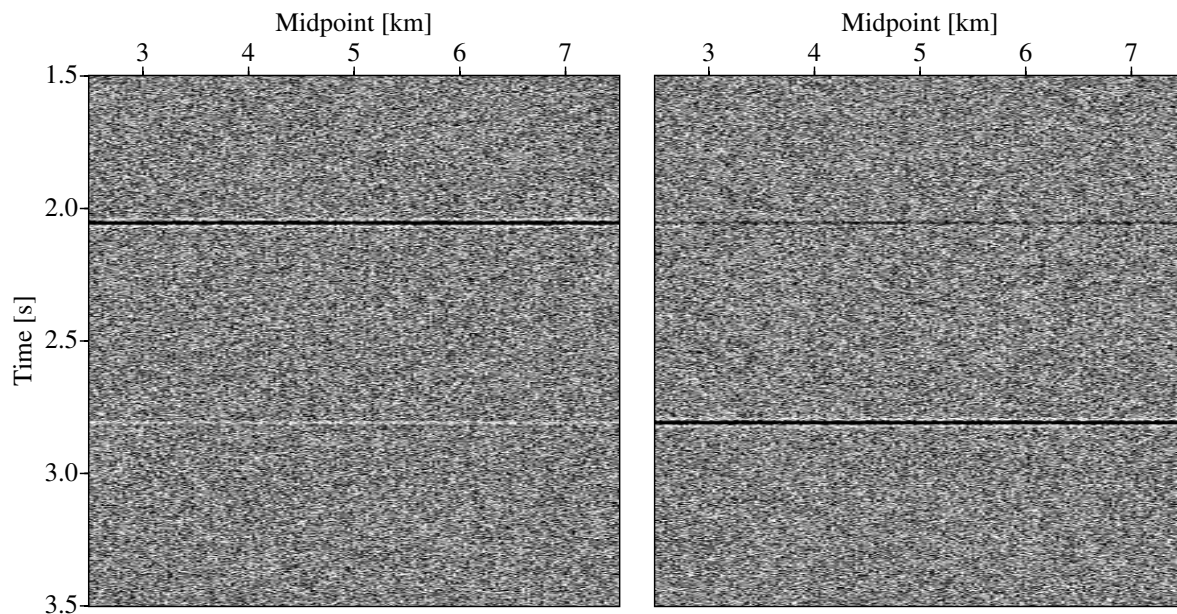


Figure 2: CO section for half-offset $h = 500$ m extracted from the synthetic prestack data: vertical (left) and horizontal (right) component. Both events can be observed on both components, the upper event is the PP reflection, the lower the PS reflection.

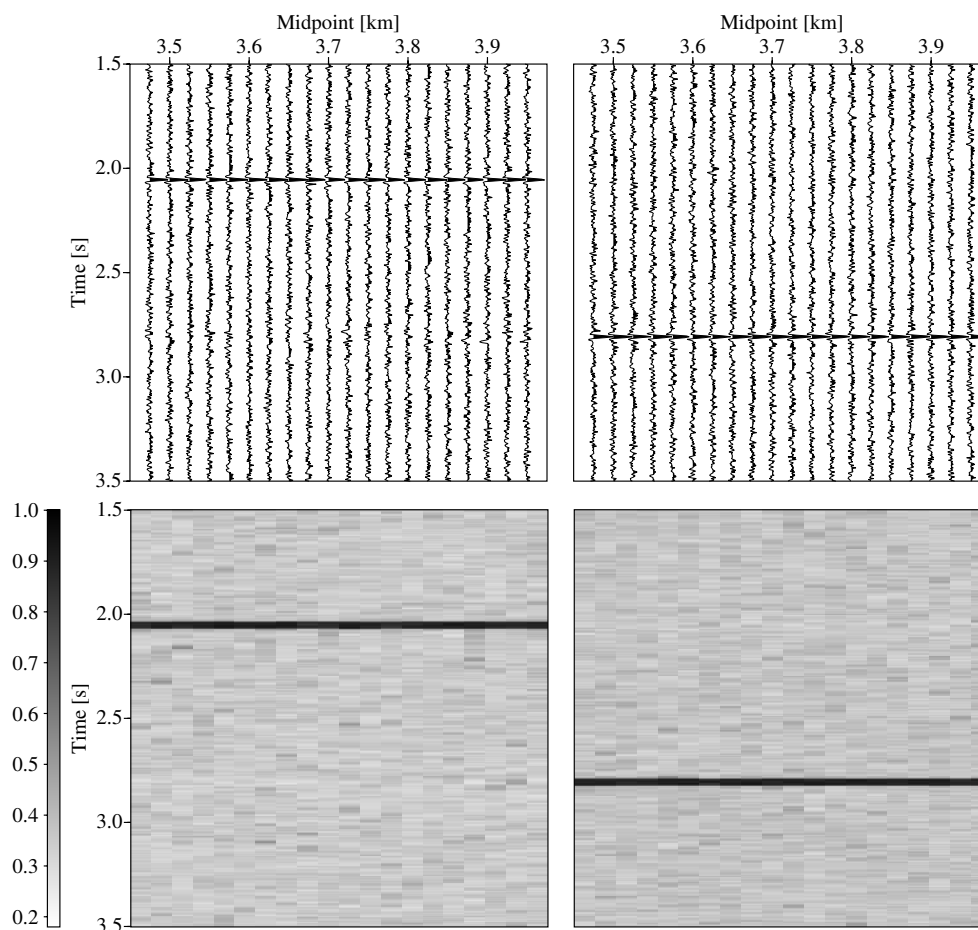


Figure 3: Subset of the CS stack for PP (left) and PS (right) reflection events simulated for half-offset $h = 500$ m. The corresponding coherence sections are displayed below. Note the clear separation of both wave types already after this first processing step.